Interface and bulk magnetization dynamics in biaxial Fe/Cr structures induced by ultrashort optical pulses

A. A. Rzhevsky, B. B. Krichevtsov, D. E. Bürgler, and C. M. Schneider

Citation: Journal of Applied Physics **104**, 083918 (2008);
View online: https://doi.org/10.1063/1.3005884
View Table of Contents: http://aip.scitation.org/toc/jap/104/8
Published by the American Institute of Physics

Interface and bulk magnetization dynamics in biaxial Fe/Cr structures induced by ultrashort optical pulses

A. A. Rzhevsky,[1,2,a)] B. B. Krichevtsov,[2] D. E. Bürgler,[1] and C. M. Schneider[1]
[1]*Institut für Festkörperforschung (IFF-9) and JARA-FIT, Forschungszentrum Jülich GmbH, D-52425 Jülich, Germany*
[2]*Ioffe Physical Technical Institute, Russian Academy of Sciences, 194021 St.Petersburg, Russia*

(Received 26 June 2008; accepted 4 September 2008; published online 31 October 2008)

The interface and bulk magnetization dynamics of single-crystalline, wedge-shaped Fe(001) thin films with Cr cap layers have been studied by time-resolved magneto-optical Kerr effect (MOKE) and time-resolved magnetization-induced second harmonic generation (MSHG) using an all-optical pump-probe technique. We observed long-lived (≈ 1 ns) MOKE and MSHG oscillations excited by ultrashort (≈ 150 fs) optical pulses. They exhibit the same main resonance frequency f and damping constant. However, a 90° phase shift was observed between linear and nonlinear responses proving that MOKE and MSHG oscillations are related to the temporal variations of different magnetization components M_z and M_y. Additionally, we found weak oscillations at the double frequency $2f$. Comparing the results of static and dynamic MSHG measurements we evaluate the in-plane amplitude of the optically excited interfacial magnetization oscillations. © *2008 American Institute of Physics*. [DOI: 10.1063/1.3005884]

I. INTRODUCTION

Currently, the issue of magnetization dynamics is intensely studied both in thin magnetic films and bulk crystals. Of particular interest is the dynamic response induced by ultrashort optical pulses.[1–5] The practical interest in this type of excitation mechanism is driven by the possibility of ultrafast optical switching of local magnetic areas, which might be used for the development of new types of optomagnetic devices for information and data processing technology. From a more fundamental point of view this optical approach allows us to investigate the microscopic mechanisms governing the excitation of magnetization dynamics on a very short time scale and to test the applicability, the limits, and validity of the classical Landau–Lifshitz–Gilbert (LLG) formalism.

Epitaxial Fe/Cr and Fe/Cr/Fe structures are well known with respect to their magnetic properties and have been studied by a variety of different methods [ferromagnetic resonance (FMR), Brillouin light scattering (BLS), magneto-optical Kerr effect (MOKE)].[6–8] Since the discovery of giant magnetoresistance (GMR)[9,10] Fe/Cr is considered as a model system of the physics of ferromagnetism in reduced dimensions. One of its particular features is a fourfold or biaxial in-plane magnetic anisotropy. In Ref. 11 using an all-optical pump-probe approach on the basis of the linear time-resolved MOKE (TR-MOKE), a long-living magnetization precession was excited and investigated in such biaxial Fe/Cr films with a magnetic field applied in the film plane. In these previous experiments we have shown that the oscillation frequency, excitation efficiency, angle, and field variations of the magnetization oscillations are determined by the magnetic anisotropy parameters, orientation, and magnitude of the magnetic field, and that they may be satisfactorily described taking into account the excitation of a uniform precessional mode.

It is important to realize that the magnetization dynamics probed by the TR-MOKE method reflects basically the properties of the bulk magnetization. The reason is that the magnitude of the Kerr effect stems from a signal accumulated along the entire thickness of the film, provided the latter is smaller than the information depth of the light. The dynamic behavior of the interfacial magnetization, however, is usually masked by the bulk signal in this approach. In order to probe the interface magnetization selectively, a different technique is needed. This can be obtained by means of time-resolved magnetization-induced second-harmonic generation (TR-MSHG).[12,13] In this method a pulsed pump beam excites the magnetization precession and a femtosecond probe pulse is used to generate a magnetic second harmonic generation (MSHG) signal, the amplitude of which depends on the transient magnetic state at a time delay Δt after the excitation. It is known that SHG as well as magnetic SHG in magnetic thin films and multilayers with centrosymmetric structure originates from a very narrow region of 1 or 2 ML (monolayer) at the surface or interface. In this region the inversion symmetry is broken and, therefore, the generation of a electrodipole second harmonic radiation is allowed.[14] An analysis of this MSHG signal gives a selective access to the magnetodynamic response at the interfaces.

The investigation of MSHG in exchange coupled Fe/Cr/Fe and Fe/Cr structures[15] showed that for incidence angles close to the surface normal the nonlinear response in different polarization combinations (pp,ss,ps,sp) is related to different in-plane interfacial magnetization components. This feature can be exploited to investigate not only the static but particularly also the dynamical behavior of different in-plane magnetization components at the interface. It

a)Electronic mail: rzhev@mail.ioffe.ru.

should be noted, however, that although the TR-MOKE method allows one to quite precisely extract the frequencies and damping of the magnetization oscillations in wide range of magnetic fields, the absolute values of the oscillation amplitudes can only be determined approximately. This limitation is related to the fact that the rotation of the polarization plane of the reflected probe beam in these experiments is due to the polar Kerr effect and is thus defined mainly by oscillations of the magnetization component normal to the film plane M_z. At the same time the amplitude of the out-of-plane magnetization oscillations is much smaller than those taking place in the film plane. Due to the strong demagnetizing fields in a thin film the magnetization vector oscillates on strongly elongated elliptical trajectories. Therefore, the amplitude of the magnetization oscillations in the film plane might be determined only approximately based on theoretical estimations of the ellipticity of magnetization trajectory. The combination of static MSHG and dynamical TR-MSHG measurements, on the other hand, gives the possibility to specifically evaluate the amplitude of the oscillations of in-plane magnetization components.

The TR-MSHG has been employed to study subnanosecond magnetization dynamics in Permalloy,[16] Ni and Co films on Cu(001),[17] antiferromagnetic Cr_2O_3,[18] and NiO,[19] Gd thin films,[20,21] and exchange-biased Mn/Co films.[22] In Refs. 23–25 MOKE, MSHG, as well as TR-MOKE and TR-MSHG methods were used to investigate the switching process and the bulk and interfacial magnetization dynamics in epitaxial AlGaAs/Fe films. It was shown that the switching of the magnetization as well as the magnetization dynamics, i.e., the resonance frequencies of the free magnetization precession, may differ in the bulk and at the interface. This finding was interpreted as an indication that the interfacial and bulk magnetization contributions in AlGaAs/Fe may be to some extent decoupled. This interesting result immediately raises several questions: in which way is the interface magnetic anisotropy transmitted to the bulk, what is the Curie temperature of a quasi-two-dimensional interface, is the decoupling of the bulk and interfacial magnetizations a specific feature of AlGaAs/Fe films or it is a general property of epitaxial Fe films, and what is the microscopic origin of such a weak coupling?

In this work we employed both TR-MOKE and TR-MSHG methods to study interfacial and bulk magnetization dynamics induced by ultrafast laser pulses in epitaxial GaAs(100)/Ag/Fe/Cr structures. Additionally, the static field dependencies of the MSHG response were measured at the same experimental conditions allowing us to extract the nonlinear optical susceptibilities necessary for the numerical analysis of the results. We show that in Fe/Cr films the oscillations of the interfacial and bulk magnetizations occur at the same frequency f, which also corresponds to the uniform mode frequency. The presence of a weak frequency-doubled ($2f$) component in the Fourier spectrum may be associated with a nonlinear dependence of the SHG signal ($I_{2\omega}$) on the azimuth of interfacial magnetization. The 90° phase shift between the TR-MSHG and TR-MOKE oscillations confirms that the oscillations are caused by in-plane and out-of-plane magnetization components, respectively, with the magnetization vector oscillating on strongly elliptical trajectories with a large in-plane axis. Based on the comparison of the MSHG field dependencies with TR-MSHG data the amplitude of the in-plane magnetization oscillations is estimated to about 13°.

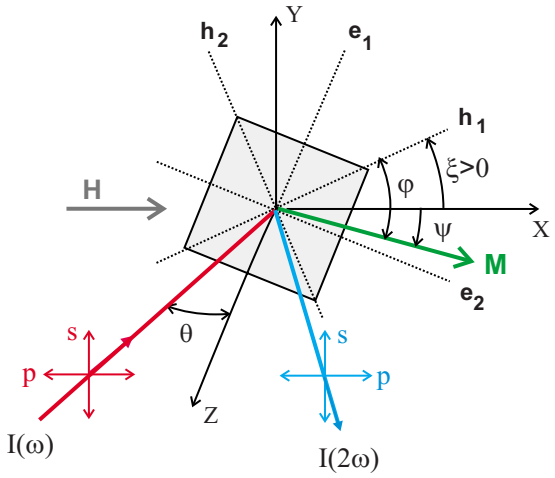

FIG. 1. (Color online) Geometry of the all-optical TR-MOKE and SHG pump-probe experiment for a fourfold anisotropic system: Here, the ($\mathbf{h_1}$,$\mathbf{h_2}$) hard and ($\mathbf{e_1}$,$\mathbf{e_2}$) easy axes correspond to the [110] and [100]-type crystallographic directions in the Fe film plane, respectively. X,Y,Z is a laboratory coordinate system; **H** the external field; ξ: azimuth of the hard axis $\mathbf{h_1}$; φ: angle between magnetization **M** and hard axis $\mathbf{h_1}$; ψ: azimuthal angle of **M**; θ: angle of incidence.

II. EXPERIMENTAL ASPECTS

Wedge-shaped Fe films (thickness $d=10-50$ nm) were grown by molecular beam epitaxy onto GaAs(001) substrates, with a Ag (150 nm)/Fe (1 nm) buffer layer being deposited prior to the Fe film growth in order to provide better epitaxy.[26] The structure was covered by a Cr (2 nm) protective cap layer. The quality of the films has been monitored *in situ* by reflection high-energy electron diffraction during the growth process. Both Fe and Cr layers crystallize in the bcc structure, which for Fe gives rise to cubic magnetocrystalline anisotropy. The strong demagnetizing field of the thin film geometry confines the static magnetization for our film thicknesses predominantly in the film plane even in the presence of positive interface anisotropy contributions (easy axis parallel to the surface normal) at the Fe/Ag and Fe/Cr interfaces. Therefore, the overall magnetic anisotropy of the Fe layers can be described by an effective in-plane, fourfold anisotropy energy.

After deposition the sample was removed from the chamber and mounted onto a sample holder allowing a 360° rotation around the surface normal. All measurements were performed at room temperature ($T=294$ K). The geometry of the experiment and the definitions of the angles are given in Fig. 1.

The dynamic response of the magnetization **M** resulting in TR-MSHG and TR-MOKE signals was induced by short 150 fs pump-light pulses at $\lambda=800$ nm ($E_{\mathrm{ph}}=\hbar\omega=1.55$ eV) generated by a regenerative amplifier (Spitfire-Pro, SpectraPhysics) with 1 kHz repetition rate at the normal incidence. In the case of TR-MSHG a photon counting technique was employed to record the pump-pulse-induced SHG

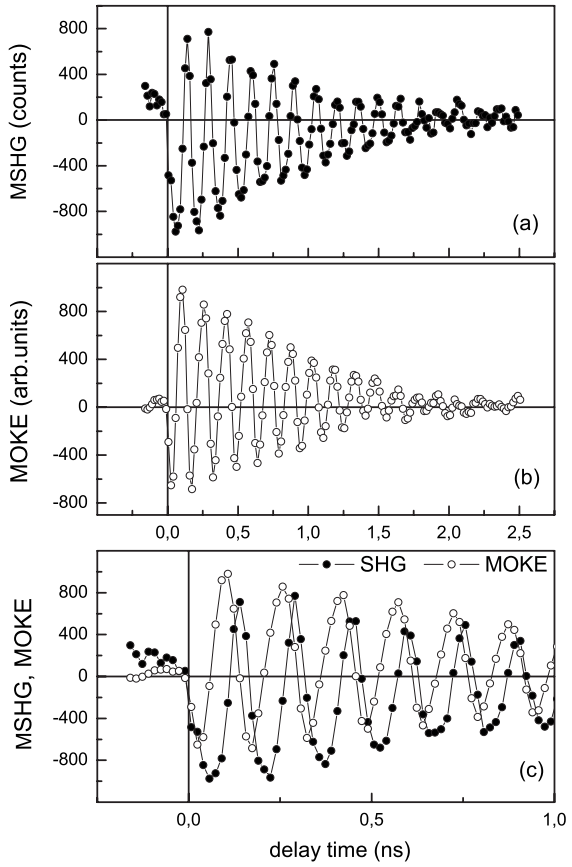

FIG. 2. Time profiles of (a) the MSHG and (b) the Kerr rotation in *pp* polarization combination for a Fe (26 nm)/Cr (2 nm) bilayer at $H=0.5$ kOe and $\xi=2°$: A constant offset of about 2500 counts is subtracted in (a) for clarity. (c) TR-MOKE and TR-MSHG signals on an expanded time scale reveal a 90° phase shift.

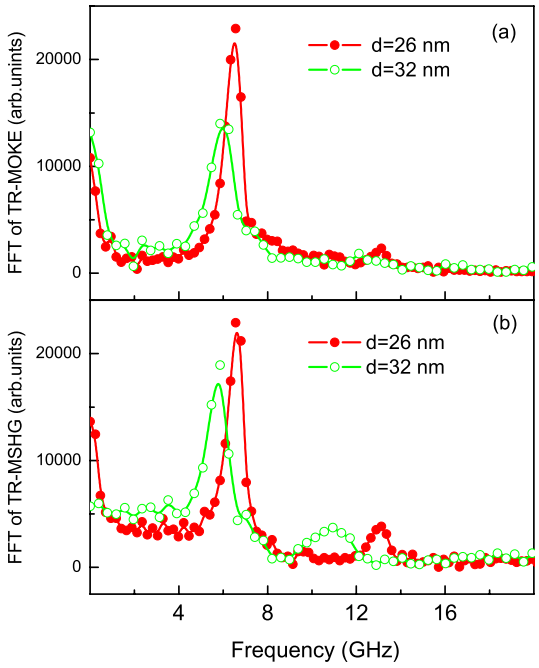

FIG. 3. (Color online) Fourier transforms of the (a) TR-MOKE and (b) TR-MSHG signals for Fe (26 nm)/Cr (2 nm) and Fe (32 nm)/Cr (2 nm) films measured under the same conditions as in Fig. 2.

intensity changes of the probe beam at the double frequency $\lambda=400$ nm ($E_{ph}=2\hbar\omega=3.10$ eV). The fundamental light at $\lambda=800$ nm was rejected by placing a blue filter (BG-39) into the reflected beam. The counting time of each experimental point was set to 10–20 s. In the case of TR-MOKE, a lock-in technique and differential photodetector were used to measure the pump-pulse-induced polarization plane rotation changes in the probe beam. In both approaches the probe beam incidence angle was fixed at $\theta\approx 10°$. The diameters of the surface illuminated area were ≈ 1 and ≈ 0.3 mm with an average power of 10 and 3 mW for the pump and probe beam, respectively. The measurements of TR-MSHG and TR-MOKE were carried out at a magnetic field of 0.5 kOe oriented close to a hard axis direction ($\xi=2°$), since at this field value and orientation the maximal amplitude of the coherent magnetization oscillations has been observed.[11] In addition, the nonuniform magnetic structure due to domains having opposite projections of **M** on the y axis is also absent.[27]

The static MSHG and MOKE field dependencies were measured in magnetic fields up to 3 kOe applied parallel to the sample surface in the plane of incident light (*longitudinal geometry*). It is important to note that both TR-MSHG and MSHG measurements were performed at the same experimental conditions, i.e., using the same experimental setup with the same light excitation power, incident angles, and polarization of the probe beam used to obtain the MSHG signal.

III. EXPERIMENTAL RESULTS

In Figs. 2(a) and 2(b) the MOKE and MSHG intensity versus time profiles on an Fe (26 nm)/Cr (2 nm) film for the *pp* polarization combination are shown. The data have been recorded at an in-plane magnetic field $H=0.5$ kOe and an azimuth angle of $\xi=2°$ relative to the hard axis. For reasons of convenience a constant offset of ~2500 counts is subtracted. The main magnetization oscillations in both TR-MOKE and TR-MSHG signals take place at the same frequency $f=6.5$ GHz. In addition, they are characterized by quite similar values of the damping parameter. At the same time—as follows from Fig. 2(c)—the TR-MSHG and TR-MOKE oscillations have a phase shift of ~90°. Analogous results (not shown here) were obtained at different iron layer thicknesses.

In Figs. 3(a) and 3(b) the fast Fourier transform (FFT) results for the MOKE and MSHG time profiles in Fe (26 nm)/Cr (2 nm) and Fe (32 nm)/Cr (2 nm) films are shown. The direction and magnitude of the magnetic field are the same as in Fig. 2. As one can see the Fourier spectrum of the TR-MOKE signal shows the presence of strong oscillations at the main frequency $f=6.5$ GHz [Fe (26 nm)] and $f=5.9$ GHz [Fe (32 nm)], which corresponds to the frequency of the uniform precession mode. Furthermore, we observe very weak oscillations close to the noise level at the double frequency $2f$. In contrast to this behavior, the oscillations at doubled frequency can be clearly discerned in the Fourier spectrum of the TR-MSHG response. The $2f$ amplitude is only five times smaller than the oscillations occurring on the main frequency f. The (≈1 GHz) shift of the main fre-

quency to higher values between the Fe (26 nm) and Fe (32 nm) films might be caused by the change in the effective in-plane magnetic anisotropy K_1 due to an increase in the interfacial contribution to K_1 as the film becomes thinner. Another possible reason may be a minute uncertainty in the position of the azimuthal angle ψ, because at $H=0.5$ kOe the resonance frequency f drastically depends on ψ.

Thus, in our GaAs(001)/Ag/Fe/Cr films at the experimental conditions chosen, we find that the values of main oscillation frequencies f measured by TR-MSHG and TR-MOKE agree within the experimental uncertainty. The phase of these oscillations, however, differs by 90°. The remarkable oscillations at $2f$ also appear in the Fourier spectrum of the TR-MSHG response, while they are only very weak in the Fourier spectrum of TR-MOKE signal.

IV. CALCULATIONS AND DISCUSSION

For the analysis of the experimental results we use expressions linking the MSHG intensity in different polarization combinations with components of the interfacial magnetization **M**.[15,28–30] We follow the arguments given in Ref. 15, which base the analysis on the use of effective nonlinear susceptibilities χ_{ijk}^{eff} accounting for (i) possible differences between the top and bottom interfaces, (ii) light absorption at the frequencies ω and 2ω, and (iii) angle of incidence close to the surface normal ($\theta \approx 10°$). Using this approach, the expression for the nonlinear response in *pp* polarization combination for a C_{4v} point symmetry group [(100)-type surface] has a form[15]

$$I_{2f} = A|\chi_{xxx}^{\text{eff}} M_y + \alpha_n \theta|^2 = A\{|\chi_{xxx}^{\text{eff}}|^2 M_y^2 + |\alpha_n \theta|^2 + 2|\chi_{xxx}^{\text{eff}} t| \times |\alpha_n| \theta M_y \cos\Delta\}, \quad (1)$$

where A is a parameter depending on the intensity of the fundamental light; χ_{xxx}^{eff} is odd in **M** and $\alpha_n = [2\chi_{zx}^{\text{eff}}/n + N\chi_{zxx}^{\text{eff}}]$ is the nonmagnetic contribution to the nonlinear response, respectively; n and N are refraction indices at ω and 2ω; θ is the incidence angle; Δ is the phase shift, since χ_{xxx}^{eff} and α_n are complex numbers.

As it follows from Eq. (1), the MSHG intensity for the *pp* polarization combination is defined by the M_y interfacial magnetization component and contains both linear and quadratic on M_y contributions. To define the values of the parameters entering into Eq. (1), we investigated the field dependencies of the MSHG presponse in *pp* configuration. Equation (1) can be used to describe the experimental field dependencies of the MSHG signal, provided the changes in the M_x and M_y components depending on the magnitude and direction of the applied magnetic field **H** are known.

To calculate the M_x and M_y field dependencies the following expression for the magnetic energy density ϵ_m may be used:

$$\varepsilon_m = -HM_s \cos\psi + \frac{K_1}{4}\cos^2(2\varphi), \quad (2)$$

where the first and second terms correspond to the Zeeman and fourfold in-plane magnetic anisotropy energies, respectively. M_s is the saturation magnetization; K_1 is the magnetic anisotropy constant; ψ is the angle between magnetization **M** and magnetic field **H**; φ is the angle between **M** and the hard axis $\mathbf{h_1}$ (see Fig. 1). The saturation magnetization value $M=1.71$ kG of bulk Fe and the expression $2K_1/M_s = [0.55-2.5/d(ML)]$ kOe (Ref. 6) to define the anisotropy constant have been used in the calculations of ϵ_m. The minimization of Eq. (2) allows us to define the equilibrium orientation of the magnetization **M** in the film plane depending on the direction and magnitude of the applied magnetic field **H**. The parameters $A|\chi_{xxx}^{\text{eff}}|^2$, $A|\alpha_n\theta|^2$, and $2A|\chi_{xxx}^{\text{eff}}||\alpha_n\theta|\cos\Delta$ can then be determined from the experimental values $I_{2\omega}(H \to +0)$, $I_{2\omega}(H \to -0)$, and $I_{2\omega}(\pm H_s)$ for the corresponding *pp* polarization combination. In Figs. 4(a) and 4(b) the experimental and calculated MSHG field dependencies are shown.

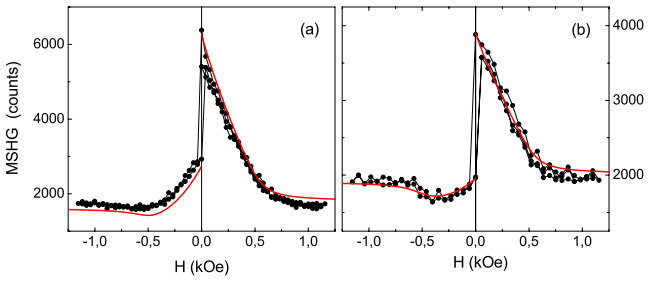

FIG. 4. (Color online) Magnetic field dependence of the MSHG intensity in (a) Fe (26 nm) and (b) Fe (34 nm) films: The red line shows calculations using Eq. (1) at the following set of parameters $A|\chi^{\text{eff}}|^2=5600$ (counts), $A|\alpha_n\theta|^2=1700$ (counts), $2A|\chi^{\text{eff}}||\alpha_n\theta|\cos\Delta=2490$ (counts) for Fe (26 nm) film and $A|\chi^{\text{eff}}|^2=1920$ (counts), $A|\alpha_n\theta|^2=1960$ (counts), $2A|\chi^{\text{eff}}||\alpha_n\theta|\cos\Delta=1360$(counts) for Fe (34 nm) film.

Since the static field dependencies and laser pulse-induced time-dependent variations of the MSHG response were measured at the same experimental conditions the fit parameters describing the static field variations of the MSHG signal may also be used to calculate the amplitude and Fourier spectra of the TR-MSHG oscillations. The results of the calculations are shown in Fig. 5. In fact, the MSHG changes for both static and dynamic measurements are caused by magnetization rotations, except that in the first case the (slow) magnetization rotation is due to external magnetic field, while in the second case the (fast) rotation is caused by the free magnetization oscillations. In Fig. 5(a) the experimental and calculated [by use of Eq. (1)] time variations of the MSHG signal for the Fe (26 nm) film are shown. The calculations were performed assuming that the azimuthal angle of the magnetization ψ is varying with time t according to the equation:

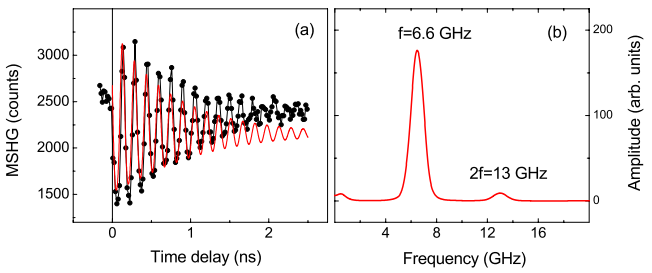

FIG. 5. (Color online) (a) Experimental (black) and calculated (red) temporal MSHG intensity variations in Fe (26 nm) film after applying an ultrashort laser pulse: The calculations are performed using Eq. (1) and the parameters obtained by fitting the static MSHG field dependencies shown in Fig. 4. (b) Fourier spectrum of the calculated time profile in (a).

$$\psi(t) = \psi(H) + \psi_0 \exp(-\alpha t)\cos(2\pi f t + \phi), \quad (3)$$

where $\psi(H)$—an equilibrium azimuth of the magnetization at the field H, ψ_0-amplitude of oscillations, α—damping, $f = 6.5$ GHz-oscillation frequency, ϕ—initial phase of oscillations.

The best agreement between the experimental and calculated field variations is obtained at a maximum amplitude of the oscillations of $\psi_0 = 13°$. The large amplitude value means that at the excitation power given the system may be already at the threshold of the applicability of the LLG equations. As it is known, these equations are linearized and only valid for small deflections $\mathbf{m}_\sim$ of the magnetization vector from the equilibrium value, i.e., $\mathbf{m}_\sim \ll \mathbf{M}$. When the oscillation amplitude takes a significant value, i.e., $\psi_0 > 10°$, the linearized LLG equations will give only approximate solutions. At a deflection angle of 13° from the equilibrium orientation the magnitude of $\mathbf{m}_\sim$ is about 22% of $\mathbf{M}$, i.e., only five times smaller than $\mathbf{M}$ and effects of higher order (nonlinear) may be expected.

The Fourier spectrum [Fig. 5(b)] of the calculated MSHG oscillations shown in Fig. 5(a) displays a strong first harmonic and a much weaker $2f$ second harmonic contribution. The appearance of oscillations at a frequency of $2f$ for the calculated TR-MSHG, as it follows from Eq. (1), is due to a nonlinearity of the $I_{2\omega}$ function. The relation (A_{2f}/A_f) between the amplitudes of the $2f$ and f frequency contributions is about 0.05. The same relation (A_{2f}/A_f) obtained from the experimental data [Fig. 3(b)], however, is about three times larger. This discrepancy suggests that the optical nonlinearity involved in Eq. (1) is not the only reason for the appearance of a $2f$ TR-MSHG signal and, most probably, a magnetic nonlinearity (beyond the linearized LLG equations) should be also taken into account. For example, a dependence of the damping on the intensity of the laser excitation pump pulse in CrO_2 films was recently reported in Ref. 31. It seems that the explanation of this phenomenon must include higher order expansions in the description of the magnetization dynamics as compared to the linearized LLG equations.

The phase shift observed between the MOKE and MSHG oscillations (Fig. 2) is a clear evidence that the linear response relates to the polar Kerr effect and is caused by time variations of the magnetization component normal to the film plane. On the other hand, the nonlinear response is related to changes in the in-plane magnetization component. Since the oscillations happen on strongly elongated elliptical trajectories around of the effective field $\mathbf{H}_{\text{eff}}$ oriented in the film plane, the phase shift between the two effects should be 90° as observed in the experiment.

V. CONCLUSIONS

Our investigations show that in GaAs(001)/Ag/Fe/Cr—in contrast to AlGaAs/Fe films—the oscillations of the interfacial and bulk magnetizations appear at the same frequency corresponding to the uniform precessional mode. Besides, the field dependencies of the MOKE and MSHG in the Fe/Cr films can be described using the same magnetic potential. This means that in these structures the interfacial and bulk magnetization behave in a very similar way with respect to both their static and dynamic response.

In view of our findings on the Fe/Cr films, the different behaviors of the interfacial and bulk magnetization observed previously in AlGaAs/Fe films must be discussed. A possible cause for this discrepancy may be related to the different natures of the samples, i.e., the properties of the interface between a metal and semiconductor (AlGaAs/Fe) and between two metals (Ag/Fe and Fe/Cr). In the former case the interface is formed by a metal and semiconductor having a different O_h and T_d bulk crystalline structure, while in the latter case the interface is formed by different metals having the same O_h bulk structure. In addition to these structural differences, the semiconductor/metal interface has a stronger tendency for intermixing, which can have a significant influence on the magnetic properties in the entire interface-near region. For example, the interdiffusion of As into Fe is known to reduce the magnetic moment.[32] In this way, a zone of reduced magnetization may be formed at the interface, which may also exhibit a reduced exchange coupling to the bulk of the film. Such a mechanism may explain the observations in the AlGaAs/Fe system. Clearly further investigations will be needed to shed more light onto the microscopic origin of this phenomenon.

The second main result of our work consists in the experimental determination of absolute values for the amplitude of the optically excited magnetization oscillations in the film plane. The large amplitude of the oscillations observed $(\psi_0 \approx 13°)$ gives evidence that the dynamical behavior of the system is at the limit of the applicability of the linearized LLG approach and higher order effects should be included in the analysis of the results.

ACKNOWLEDGMENTS

The authors would like to thank R. Schreiber for the sample preparation.

[1] E. Beaurepaire, J.-C. Merle, A. Daunois, and J.-Y. Bigot, Phys. Rev. Lett. **76**, 4250 (1996).
[2] B. Koopmans, M. van Kampen, J. T. Kohlhepp, and W. J. M. de Jonge, Phys. Rev. Lett. **85**, 844 (2000).
[3] Y. Acremann, M. Buess, C. H. Back, M. Dumm, G. Bayreuther, and D. Pescia, Nature (London) **414**, 51 (2001).
[4] I. Tudosa, C. Stamm, A. B. Kashuba, F. King, H. C. Siegmann, J. Stöhr, G. Ju, B. Lu, and D. Weller, Nature (London) **428**, 831 (2004).
[5] A. Kimel, A. Kirilyuk, and Th. Rasing, Proc. SPIE **6892**, 68920P (2008).
[6] B. Heinrich and J. F. Cochran, Adv. Phys. **42**, 523 (1993).
[7] R. J. Hicken, S. J. Gray, A. Ercole, C. Daboo, D. J. Freeland, E. Gu, E. Ahmad, and J. A. C. Bland, Phys. Rev. B **55**, 5898 (1997).
[8] D. E. Bürgler, P. Grünberg, S. O. Demokritov, and M. T. Johnson, in *Handbook of Magnetic Materials*, edited by K. H. J. Buschow (Elsevier Science, New York, 2001), Vol. 13.
[9] M. N. Baibich, J. M. Broto, A. Fert, F. Nguyen Van Dau, F. Petroff, P. Etienne, G. Creuzet, A. Friederich, and J. Chazelas, Phys. Rev. Lett. **61**, 2472 (1988).
[10] G. Binasch, P. Grünberg, F. Saurenbach, and W. Zinn, Phys. Rev. B **39**, 4828 (1989).
[11] A. A. Rzhevsky, B. B. Krichevtsov, D. E. Bürgler, and C. M. Schneider, Phys. Rev. B **75**, 224434 (2007).
[12] J. Hohlfeld, U. Conrad, J. G. Müller, S.-S. Wellershoff, and E. Matthias, in *Nonlinear Optics in Metals*, edited by K. H. Bennemann (Clarendon, Oxford, 1998).

[13]T. Luce and K. H. Bennemann, in *Nonlinear Optics in Metals*, edited by K. H. Bennemann (Clarendon, Oxford, 1998).
[14]Y. R. Shen, *The Principles of Nonlinear Optics* (Wiley, New York, 1984).
[15]A. A. Rzhevsky, B. B. Krichevtsov, D. E. Bürgler, and C. M. Schneider, Phys. Rev. B **75**, 144416 (2007).
[16]T. M. Crawford, T. J. Silva, C. W. Teplin, and C. T. Rogers, J. Appl. Phys. **74**, 3386 (1999).
[17]J. Güdde, U. Conrad, V. Jähnke, J. Hohlfeld, and E. Matthias, Phys. Rev. B **59**, R6608 (1999).
[18]T. Satoh, B. B. Van Aken, N. P. Duong, T. Lottermoser, and M. Fiebig, Phys. Rev. B **75**, 155406 (2007).
[19]N. P. Duong, T. Satoh, and M. Fiebig, Phys. Rev. Lett. **93**, 117402 (2004).
[20]M. Lisowski, P. A. Loukakos, A. Melnikov, I. Radu, L. Ungureanu, M. Wolf, and U. Bovensiepen, Phys. Rev. Lett. **95**, 137402 (2005).
[21]A. Melnikov, I. Radu, U. Bovensiepen, O. Krupin, K. Starke, E. Matthias, and M. Wolf, Phys. Rev. Lett. **91**, 227403 (2003).
[22]V. K. Valev, A. Kirilyuk, F. Dalla Longa, J. T. Kohlhepp, B. Koopmans, and Th. Rasing, Phys. Rev. B **75**, 012401 (2007).
[23]H. B. Zhao, D. Talbayev, G. Lüpke, A. T. Hanbicki, C. H. Li, and B. T. Jonker, Appl. Phys. Lett. **91**, 052111 (2007).
[24]H. B. Zhao, D. Talbayev, Q. G. Yang, G. Lüpke, A. T. Hanbicki, C. H. Li, O. M. J. van 't Erve, G. Kioseoglou, and B. T. Jonker, Appl. Phys. Lett. **86**, 152512 (2005).
[25]H. B. Zhao, D. Talbayev, G. Lüpke, A. T. Hanbicki, C. H. Li, M. J. van 't Erve, G. Kioseoglou, and B. T. Jonker, Phys. Rev. Lett. **95**, 137202 (2005).
[26]D. E. Bürgler, C. M. Schmidt, D. M. Schaller, F. Meisinger, R. Hofer, and H.-J. Güntherodt, Phys. Rev. B **56**, 4149 (1997).
[27]A. A. Rzhevsky, B. B. Krichevtsov, D. E. Bürgler, and C. M. Schneider, Phys. Rev. B **77**, 174432 (2008).
[28]W. Hübner and K. H. Bennemann, Phys. Rev. B **52**, 13411 (1995).
[29]R. Atkinson and N. F. Kubrakov, Phys. Rev. B **65**, 014432 (2001).
[30]L. C. Sampaio, J. Hamrle, A. Mougin, J. Ferré, F. Garcia, F. Fettar, B. Dieny, and A. Brun, Phys. Rev. B **70**, 104403 (2004).
[31]G. M. Müller, M. Münzenberg, G.-X. Miao, and A. Gupta, Phys. Rev. B **77**, 020412(R) (2008).
[32]C. A. F. Vaz, J. A. C. Bland, and G. Lauhoff, Rep. Prog. Phys. **71**, 056501 (2008).